Jurnal Teknologi

Full paper

Robust Stabilizing Controller Design for Inverted Pendulum System

Hazem I. Ali*

Control and Systems Engineering Department, University of Technology, Baghdad-Iraq

*Corresponding author: hazem.i.ali@uotechnology.edu.iq

Article history

Received :5 May 2014
Received in revised form :
25 August 2014
Accepted :15 November 2014

Graphical abstract

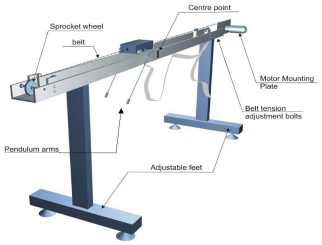

Abstract

In this paper the design of robust stabilizing state feedback controller for inverted pendulum system is presented. The Ant Colony Optimization (ACO) method is used to tune the state feedback gains subject to different proposed cost functions comprise of H-infinity constraints and time domain specifications. The steady state and dynamic characteristics of the proposed controller are investigated by simulations and experiments. The results show the effectiveness of the proposed controller which offers a satisfactory robustness and a desirable time response specifications. Finally, the robustness of the controller is tested in the presence of system uncertainties and disturbance.

Keywords: Inverted pendulum; uncertain systems; robust control; ant colony optimization

1.0 INTRODUCTION

Single inverted pendulum is a classical problem in the field of non-linear control theory; it also offers a good example for control engineers to verify a modern control theory. The inverted pendulum is a highly nonlinear and open-loop unstable system. The characteristics of the inverted pendulum make identification and control more challenging. The inverted pendulum is a benchmark underactuated, unstable and nonlinear system that is used in many control experiments to demonstrate the effectiveness of different control approaches. It is used in a manner analogous to the control of many real systems such as rockets during liftoff, bipedal walking, cranes, robots, and etc. [1, 2]. Several control strategies based on the conventional control theory, modern control theory, adaptive control and intelligent control have been used to control the inverted pendulum, such as PID controller, linear quadratic regulator (LQR), fuzzy logic controller (FLC). Furthermore, the effect of new control methods is verified using pendulum system because of the simplicity of the structure and the wealth of its nonlinear model. Further, the simple structure allows real and virtual experiments to be carried out [3, 4, 5].

On the other hand, a Single rod Inverted Pendulum consists of a freely pivoted rod, mounted on a motor driven cart. With the rod exactly centered above the motionless cart, there is no side long resultant force on the rod and it remains balanced. In principle it can stay this way indefinitely, but in practice it never does. Any disturbance that shifts the rod away from equilibrium, gives rise to forces that push the rod far there from this equilibrium point, implying that the upright equilibrium point is inherently unstable. Under no external forces, the rod would always come to rest in the downward equilibrium point, hanging down. This is called the pendant position. This equilibrium point is stable as opposed to the upright equilibrium point. The control task is to swing up the pendulum from its natural pendant position and to stabilize it in the inverted position, once it reaches the upright equilibrium point. The cart must also be homed to a reference position on the rail [6, 7].

In this work a robust state feedback controller which is a powerful tool to control linear dynamic systems is proposed to stabilize the inverted pendulum system. The robust design is more desirable because this system cannot be precisely modeled and involve some amount of uncertainty. The Ant Colony Optimization (ACO) method is used to tune the state feedback gain matrix subject to a proposed cost function. The proposed cost function combines the H-infinity constraints and time domain specifications of the system to meet at the same time the required robustness and the desired time response specifications.

2.0 METHODOLOGY

2.1 Ant Colony Optimization (ACO) Method

The Ant Colony Optimization (ACO) method is a paradigm for designing meta-heuristic algorithms for combinatorial optimization problems. The essential trait of ACO algorithms is

the combination of a priori information about the structure of a promising solution with information about the structure of previously obtained good solutions. ACO is found on the foraging behavior of ants and their indirect communication based on pheromones, and has been applied to several combinatorial problems such as job scheduling and routing optimization in data. ACO's are especially suited for finding solutions to different optimization problems. A colony of artificial ants cooperates to find good solutions, which are an emergent property of the ant's co-operative interaction. Based on their similarities with ant colonies in nature, ant algorithms are adaptive and robust and can be applied to different versions of the same problem as well as to different optimization problems. An ant searches collectively foe a good solution to a given optimization problem. Each individual ant can find a solution or at least part of a solution to the optimization problem on its own but only when many ants work together they can find the optimal solution [8, 9].

Since the optimal solution can only be found through the global cooperation of all the ants in a colony, it is an emergent result of such this cooperation. While searching for a solution the ants do not communicate directly but indirectly by adding pheromone to the environment. Based on the specific problem an ant is given a starting state and moves through a sequence of neighboring states trying to find the shortest path. It moves based on a stochastic local search policy directed by its internal state, the pheromone trails, and local information encoded in the environment. Ants use this private and public information in order to decide when and where to deposit pheromone. In most application the amount of pheromone deposited is proportional to the quality of the move an ant has made. Thus the more pheromone, the better the solution found. After an ant has found a solution, it dies; *i.e.* it is deleted from the system. ACO is depending upon the pheromone matrix $\tau = \{\tau_{ij}\}$ for the construction of good solutions. The initial values are defined as [10]:

$$\text{Set } \tau_{ij} = \tau_0 \ \forall \ (i,j) \text{ , where } \tau_0 > 0 \tag{1}$$

The probability $P_{ij}^{\ A}(t)$ of choosing a node j at node i is defined as:

$$P_{ij}^{A}(t) = \frac{[\tau_{ij}(t)]^{\alpha}[\eta_{ij}(t)]^{\beta}}{\sum_{ij\in T^A}[\tau_{ij}(t)]^{\alpha}[\eta_{ij}(t)]^{\beta}} \ ; i,j \ \in T^A; \tag{2}$$

At each generation of the algorithm, the ant constructs a complete solution using this equation, starting at source node. Where $\eta_{ij} = \frac{1}{kj}$, α and β are the constants that determine the relative influence of the pheromone values and the heuristic values on the decision of the ant respectively. T^A is the path effectuated by the ant A at a given time.

The quantity of pheromone $\Delta\tau_{ij}$ on each path may be defined as

$$\tau_{ij}^{A} = \begin{cases} \frac{L^{min}}{L^A} & \text{if } i,j \in T^A \\ 0 & \text{else} \end{cases} \tag{3}$$

where L^A represents the value of the objective function found by the ant A.
L^{min} represents the best solution carried out by the set of the ants until the current iteration.

The pheromone evaporation is a way to avoid unlimited increase of pheromone trails. Also it allows the forgetfulness of the bad choices:

$$\tau_{ij} = \rho\tau_{ij}(t-1) + \sum_{A=1}^{NA} \Delta\, \tau_{ij}{}^{A}(t) \tag{4}$$

where

$\Delta\tau_{ij}^{A}$: The quantity of pheromone on each path.

NA: Number of ants.

ρ: The evaporation rate $0 < \rho \leq 1$.

2.2 System Mathematical Model

A sketch of an inverted pendulum mounted on a motor driven cart system is shown in Figure 1. Realistically, this simple mechanical system is representative of a class of attitude control problems whose goal is to maintain the desired vertically oriented position at all times. Since the inverted pendulum is a nonlinear system, we first develop the basic balance equations for the system, put these nonlinear equations into standard state form, and then generate a linearized model of the nonlinear plant. The open loop plant is shown to be highly unstable. A simplistic approach to classical control of this system is attempted with the end result showing rather ineffective performance [11].

To develop the mathematical model for the system, the rod is assumed to be massless and that the cart mass and the point mass at the upper end of the inverted pendulum are denoted as M and m, respectively. There is an externally x-directed force on the cart, u(t), and a gravity force acts on the point mass at all times. The coordinate system chosen is defined in Figure 1, where x(t) represents the cart position and $\theta(t)$is the tilt angle referenced to the vertically upward direction. A force balance in the x-direction gives that the mass times acceleration of the cart plus the mass times the x-directed acceleration of the point mass must equal the external force on the system.

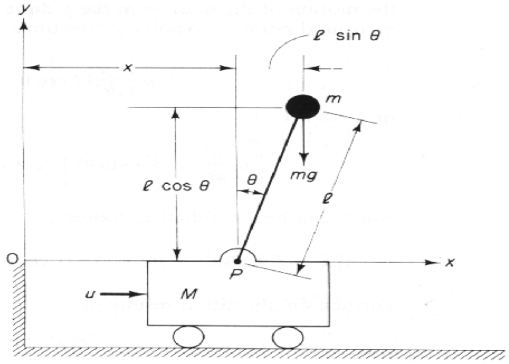

Figure 1 Inverted pendulum system

Applying Newton's second law to the x direction of motion yields [12, 13]:

$$M\frac{d^2}{dt^2}x + m\frac{d^2}{dt^2}x_g = u \tag{5}$$

where the time-dependent center of gravity of the point mass is given by the coordinates, (x_g, y_g). For the point mass assumed

here, the location of the center of gravity of the pendulum mass is simply defined as:

$$x_g = x + L\ \sin\theta\ ;\ and \quad y_g = L\ cos\ \theta \tag{6}$$

where L is the pendulum rod length. Substitution of Equation (5) into Equation (6) gives:

$$M\frac{d^2x}{dt^2} + m\frac{d^2}{dt^2}(x + Lsin\theta) = u \tag{7}$$

Noting the following definitions,

$$\frac{d}{dt}sin\theta = (cos\theta)\dot{\theta}\dot{\theta}; and\ \frac{d^2}{dt^2}sin\theta = -(sin\theta)\dot{\theta}^2 + (cos\theta)\ \ddot{\theta}$$
$$\frac{d}{dt}cos\theta = -(sin\theta)\ddot{\theta}\ ; and\ \frac{d^2}{dt^2}cos\theta = -(cos\theta)\dot{\theta}^2 \quad - (sin\theta)\ddot{\theta} \tag{8}$$

Equation (3) can be expressed as:

$$(M + m)\ddot{x} - ml(sin\theta)\dot{\theta}^2 + ml(cos\theta)\ddot{\theta} = u \tag{9}$$

Applying Newton's second law to the rotational motion, we obtain:

$$\left[m\frac{d^2}{dt^2}(x + L\sin\theta)\right]L\cos\theta - [m\frac{d^2}{dt^2}(L\cos\theta)]L\sin\theta = mgL\sin\theta$$

and this equation can be simplified as follows:

$$m[\ddot{x} - L(\sin\theta)\dot{\theta}^2 + L(\cos\theta)\ddot{\theta}]\,L\cos\theta - m[-L(\cos\theta)\dot{\theta}^2 - L(\sin\theta)\ddot{\theta}]L\sin\theta = mg\sin\theta$$

Further simplification results in:

$$m\ddot{x}\cos\theta + mL\ddot{\theta} = mg\sin\theta \tag{10}$$

Equations (9) and (10) are nonlinear differential equations. Since the inverted pendulum is wanted to be kept vertical, then $\theta(t)$ and $\theta(\dot{t})$ can be assumed small and consequently: $\sin\theta = \theta, \cos\theta = 1, and\ \theta\dot{\theta}^2 = 0$. Equations (9) and (10) can be linearized to be as follows:

$$(M + m)\ddot{x} + mL\ddot{\theta} = \tag{11}$$
$$m\ddot{x} + mL\ddot{\theta} = mg\theta \tag{12}$$

By arrangement, Equations (11) and (12) will be:

$$ML\ddot{\theta} = (M + m)g\theta - u \tag{13}$$
$$M\ddot{x} = u - mg\theta \tag{14}$$

The state variables are defined as: $x_1 = \theta, x_2 = \dot{\theta}, x_3 = x, and\ x_4 = \dot{x}$, then consequently and from Equations (13) and (14), the state space model can be expressed as:

$$\begin{bmatrix}\dot{x_1}\\ \dot{x_2}\\ \dot{x_3}\\ \dot{x_4}\end{bmatrix} = \begin{bmatrix}0 & 1 & 0 & 0\\ \frac{M+m}{Ml}g & 0 & 0 & 0\\ 0 & 0 & 0 & 1\\ -\frac{m}{M}g & 0 & 0 & 0\end{bmatrix}\begin{bmatrix}x_1\\ x_2\\ x_3\\ x_4\end{bmatrix} + \begin{bmatrix}0\\ -\frac{1}{Ml}\\ 0\\ \frac{1}{M}\end{bmatrix}u$$

$$y = \begin{bmatrix}\theta\\ x\end{bmatrix} = \begin{bmatrix}1 & 0 & 0 & 0\\ 0 & 0 & 1 & 0\end{bmatrix}\begin{bmatrix}x_1\\ x_2\\ x_3\\ x_4\end{bmatrix} \tag{15}$$

Table 1 lists the system parameters values. The nominal state space model for the system is:

$$\begin{bmatrix}\dot{x_1}\\ \dot{x_2}\\ \dot{x_3}\\ \dot{x_4}\end{bmatrix} = \begin{bmatrix}0 & 1 & 0 & 0\\ 29.8614 & 0 & 0 & 0\\ 0 & 0 & 0 & 1\\ -0.94 & 0 & 0 & 0\end{bmatrix}\begin{bmatrix}x_1\\ x_2\\ x_3\\ x_4\end{bmatrix} + \begin{bmatrix}0\\ -1.574\\ 0\\ 0.417\end{bmatrix}u$$

$$y = \begin{bmatrix}\theta\\ x\end{bmatrix} = \begin{bmatrix}1 & 0 & 0 & 0\\ 0 & 0 & 1 & 0\end{bmatrix}\begin{bmatrix}x_1\\ x_2\\ x_3\\ x_4\end{bmatrix} \tag{16}$$

Table 1 List of system parameters [14]

Parameter	Value
Gravity, *g*	9.81 m/s^2
Pole length, *l*	0.36 *m*
Cart mass, *M*	2.4 *kg*
Pole mass, *m*	0.23 *kg*

2.3 Design of State Feedback with Integral Controller

Although PID controller is a good controller for controlling the single-input-single-output (SISO) systems, only one PID controller cannot control both the cart position and the pendulum angle. On the other side, modern control theory is based on the description of system equations in terms of n^{th} first-order differential equations, and the system can be described by state space equation form. This means that only one controller can successfully stabilize the inverted pendulum system. The main design approach for systems described in state-space form is the use of state feedback, or pole placement. The first step in the pole placement design approach is to choose the locations of the desired closed loop poles. The most frequently used approach is to choose such poles based on experience in the root locus design, placing a dominant pair of closed poles and choosing other poles so that they are far to the left of the dominant closed loop poles. Another approach is based on the quadratic optimal control approach. This approach will determine the desired closed-loop poles such that it balances between the acceptable response and the amount of control energy required. Yan Lan presented a controller design based on state space pole placement method for a non-linear dynamic system described by an inverted pendulum. Huan made a comparison between several types of controller such as PID, FLC, and state feedback [15, 16].

On the other hand, when root loci are utilized for the design of control systems, the general approach may be described as that of pole placement; the poles here refer to that of the closed-loop transfer function, which are also the roots of the characteristic equation. Knowing the relation between the closed-loop poles and the system performance, we can effectively carry out the design by specifying the location of these poles. When we have a controlled process of the third order or higher, the PD, PI, single stage phase-lead, and phase-lag controllers would not be able to control independently all the poles of the system, because there are only two free parameters in each of these controllers. To investigate the condition required for arbitrary pole placement in an n^{th}-order system, let us consider that the process is described by the following state equation:

$$\frac{dx(t)}{dt} = Ax(t) + Bu(t) \tag{17}$$

where *x(t)* is an $n \times 1$ state vector, and *u(t)* is the scalar control. The state feedback control is:

$$u(t) = -Kx(t) + r(t) \tag{18}$$

where *K* is the $1 \times n$ feedback matrix with constant-gain elements, *r(t)* is the scalar reference input. By substituting Equation (18) into Equation (17), the closed-loop system is represented by the following state equation:

$$\frac{dx(t)}{dt} = (A - BK)x(t) + Br(t) \quad (19)$$

It will be shown in the following that if the pair *[A, B]* is completely controllable, then a matrix *K* exists that can give an arbitrary set of Eigen values of *(A — BK)*.
The feedback gain matrix *K* is expressed as

$$K=[K_1 \;\; K_2 \;\; \ldots\ldots \; K_n] \quad (20)$$

where $K_1, K_2, \ldots, K_n$ are real constants.

A necessary and sufficient condition for arbitrary pole placement is that the system be completely state controllable. We shall first derive the necessary condition. We begin by proving that if the system is not completely state controllable, and then there are Eigen values of matrix [*A-BK*] that cannot be controlled by state feedback. Suppose that the system of Equation (17) is not completely state controllable. Then the rank of the controllability matrix is less than n^{th} order, or

$$M = [B \vdots AB \vdots \cdots \vdots A^{n-1}B] = n \quad (21)$$

If the rank of the controllability matrix *M* is *n* (meaning that the system is completely state controllable) [17]. For the system model in Equation (16) the controllability matrix is: $M = \begin{bmatrix} 0 & -1.574 & 0 & -47.001 \\ -1.574 & 0 & -47.001 & 0 \\ 0 & 0.417 & 0 & 1.479 \\ 0.417 & 0 & 1.479 & 0 \end{bmatrix}$ (22)

The rank of the matrix *M* is: *rank* (*M*) =4=*n*.

The state feedback control structured in the preceding paragraphs has one deficiency in that it does not improve the type of the system. As a result, the state-feedback control with constant-gain feedback is generally useful only for regulator systems for which the system does not track inputs, if all the roots of the characteristic equation are to be placed at will. In general, most control systems must track inputs. One solution to this problem is to introduce integral control, just as with PI controller, together with the constant gain state feedback. The block diagram of a system with constant-gain state feedback and integral control feedback of the output is shown in Figure 2. The dynamic equations of the system are written as:

$$\frac{dx(t)}{dt} = Ax(t) + Bu(t) \quad (23)$$
$$y(t) = Cx(t) + Du(t) \quad (24)$$
$$u(t) = -Kx(t) + K_I z(t) \quad (25)$$
$$\dot{z}(\mathrm{t}) = r(t) - y(t) \quad (26)$$

where *y(t)* is the scalar output. The actuating signal *u(t)* is related to the state variables through constant state and integral feedback. The system dynamics can be described by:

$$\begin{bmatrix} \dot{x}(t) \\ \dot{z}(t) \end{bmatrix} = \begin{bmatrix} A & 0 \\ -C & 0 \end{bmatrix} \begin{bmatrix} x(t) \\ z(t) \end{bmatrix} + \begin{bmatrix} B \\ 0 \end{bmatrix} u(t) + \begin{bmatrix} 0 \\ 1 \end{bmatrix} r(t) \quad (27)$$

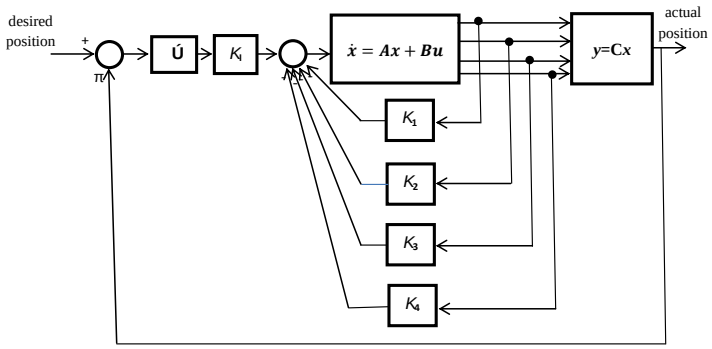

Figure 2 Block diagram of the controlled system

2.4 Tuning of State Feedback Gain Matrix Using ACO Method

In this work the ACO method is used to tune the state feedback gain matrix subject to the minimization of three different proposed cost functions. The first cost function is:

$$J_{min} = \int_0^{t_f} te^2(t)dt + \int_0^{t_f} t\theta^2(t)dt \quad (28)$$

where *e* represents the system error and t_f represents the estimated settling time of the system. This cost function is proposed to stabilize the inverted pendulum system with a desirable time response specifications for nominal parameters of the system (fixed parameters). In this case the ACO method parameters are set as: number of ants =25, the initial pheromone value=0.06, the evaporation parameter=0.4 and the number of iterations equal to 20. The resulting optimal state feedback gain matrix by ACO algorithm is:
$K_1 = -120.235,\ K_2 = -23.873, K_3 = -54.111, K_4 = -33.456,\ \ K_I = -30.523.$

The second cost function that is used to stabilize the inverted pendulum system is:

$$J_{min} = \|W_1 T + W_2 S\|_\infty \quad (29)$$

where *T* is the complementary sensitivity function which represents the relationship between the system output and desired input, *S* is the sensitivity function which represents the relationship between the system error and desired input, W_1 is the uncertainty weighting function and W_2 is the performance weighting function. This cost function represents the H-infinity constraints that satisfy the required robust stability and performance of the system with the presence of system parameters uncertainty. The uncertainty weighting function is determined to cover 10% change in system parameters. The determined uncertainty weighting function is:

$$W_1 = \frac{s+400}{0.2s+5000} \quad (30)$$

The performance weighting function is selected as a second order structure and its parameters are obtained using ACO method. The obtained performance weighting function is:

$$W_2 = \frac{0.0428s^2+2.933s+0.464}{3.076s^2-5.792s-3.014} \quad (31)$$

The ACO method parameters are set as: number of ants =25, the initial pheromone value=0.06, the evaporation parameter=0.4 and the number of iterations equal to 20. The resulting optimal state feedback gain matrix is: $K_1 = -307.968$, $K_2 = -52.620, K_3 = -191.189, K_4 = -134.289, K_I = -198.815$.

On the other hand, to achieve a more desirable time response specifications of the system with the presence of system parameters uncertainty, the following cost function is proposed:

$$J_{min} = \|W_1T + W_2S\|_\infty + \int_0^{t_f} te^2(t)dt + \int_0^{t_f} t\theta^2(t)dt \quad (32)$$

It is a combination of the time response specifications represented in Equation (28) and the H-infinity control constraints represented in Equation (29). This cost function is conducted to meet at the same time a desirable time response specifications and required robustness of the inverted pendulum system. In this case the ACO method parameters are set as: number of ants =25, the initial pheromone value=0.06, the evaporation parameter=0.4 and it is found that the selection of the number of iterations equal to 20 was fair enough and the increasing in the number of iterations did not improve the convergence of the algorithm. The resulting optimal state feedback gain matrix is: $K_1 = -240.968$, $K_2 = -66.620, K_3 = -235.189, K_4 = -134.289, K_I = -180.815$. Further, the resulting optimal performance weighting function is:

$$W_2 = \frac{0.333s^2+3.404s-0.284}{4.28s^2+1.883s+28.16} \quad (33)$$

The flowchart of ACO algorithm is shown in Figure 3.

■3.0 RESULTS AND DISCUSSION

Figure 4 shows the resulting performance of the cart position and pendulum angle when the cost function in equation (28) was applied. It is shown that the obtained time response specifications for the cart position are: $t_r = 3.2\ s, t_s = 6\ s$. The pendulum angle is stabilized in less than 5 *s* within -0.07 and 0.11 *degree*.

Figure 5 shows the resulting frequency response charactersitics of the complementary sensitivity function and sensitivity function compared with the uncertainty weighting function and performance weighting function respectively. From this figure it is clearly seen that the magnitudes of the complementary sensitivity function and sensitivity function are less than the magnitudes of the inverse of uncertainty weighting function and performance weighting function for all frequencies. This means that the robust conditions in the proposed cost function in Equation (29) have been satisfied. The obtained time response for the cart position and pendulum angle is shown in Figure 6. In this case the achieved specifications are: $t_r = 1.6\ s, t_s = 5\ s, M_p = 20\%$, and the pendulum angle oscillates between -0.1 and 0.17 *degree* and stabilized in less than 6 *s*.

Figure 7 shows the resulting frequency response charactersitics of the complementary sensitivity function and sensitivity function compared with the uncertainty weighting function and performance weighting function respectively when the proposed cost function in Equation (32) is applied. From this figure it is clearly seen that the magnitudes of the complementary sensitivity function and sensitivity function are less than the magnitudes of the inverse of uncertainty weighting function and performance weighting function for all frequencies. This means that the robust conditions have been satisfied. The obtained time response for the cart position and pendulum angle is shown in Figure 8. In this case the achieved specifications are: $t_r = 2.3\ s, t_s = 2.9\ s, M_p = 0\%$, and the pendulum angle oscillates between -0.12 and 0.2 *degree* and stabilized in less than 3.5 *s*.The control signal specifications is shown in Figure 9. It is clear that a low control effort has been obtained. The convergence rate of ACO algorithm is shown in Figure 10.

Furthermore, to test the robustness of the proposed robust controller to parameter variations, the cart mass, pole mass and pole length are varied. Figures 11 to 13 show the response of the system under different values of cart position, pole mass and pole length. It is clear that the controller can effectively compensate the parameter variations. It shows the robust performance. Further, Figure 14 shows the pendulum angle during stabilization when external disturbance is applied to the pendulum at *t*=1.9 *s*. It is shown that the pendulum angle deviates to 0.07 *degree* when the disturbance signal is introduced but the controller can accommodate the deviation and make the pendulum to maintain its upright position.

On the other hand, the real inverted pendulum used in this work is shown in Figure 15. This pendulum system consists of a cart moving along the one meter length track. The cart has a shaft to which two pendulums are attached and are able to rotate freely. The cart can move back and forth causing the pendulums to swing. The movement of the cart is caused by pulling the belt in two directions by the DC motor attached at the end of the rail. By applying a voltage to the motor, the force is controlled with which the cart is pulled. The value of the force depends on the value of the control voltage. The voltage is the control signal. The two variables that are read from the pendulum (using optical encoders) are the pendulum sway angle and the cart position on the rail. The pendulum mechanical unit interfaces with the PC through a PCI1711 interface card. The interface card reads the cart position and sway angle using two HCTL2016 incremental shaft encoders.

In order to show the practical effectiveness of the proposed controller, experiment is conducted using the real inverted pendulum system shown in Figure 15. Figure 16 shows a comparison between theoretical and experimental results. It can be seen that the proposed controller can stabilize the real inverted pendulum with approximately the same time response specifications obtained by theoretical results. Moreover, to demonstrate the effectiveness of the proposed controller, a comparison with the performance of the robust LQR controller in [6] was presented in Table 2. It is worth to note that the proposed controller can achieve a more desirable time response specifications than the LQR controller.

■4.0 CONCLUSIONS

A design of robust state feedback stabilizing controller for inverted pendulum system has been presented in this work. The state feedback gains have been tuned using ACO method subject to H-infinity constraints and time domain specifications. It was shown that the proposed controller can work sufficiently to drive the system and it is computationally efficient with the use of ACO method. In addition, the proposed controller can effectively compensate the variations in system parameters. Finally, the theoretical and experimental results showed that the proposed controller has achieved the required robustness and a desirable time response specifications.

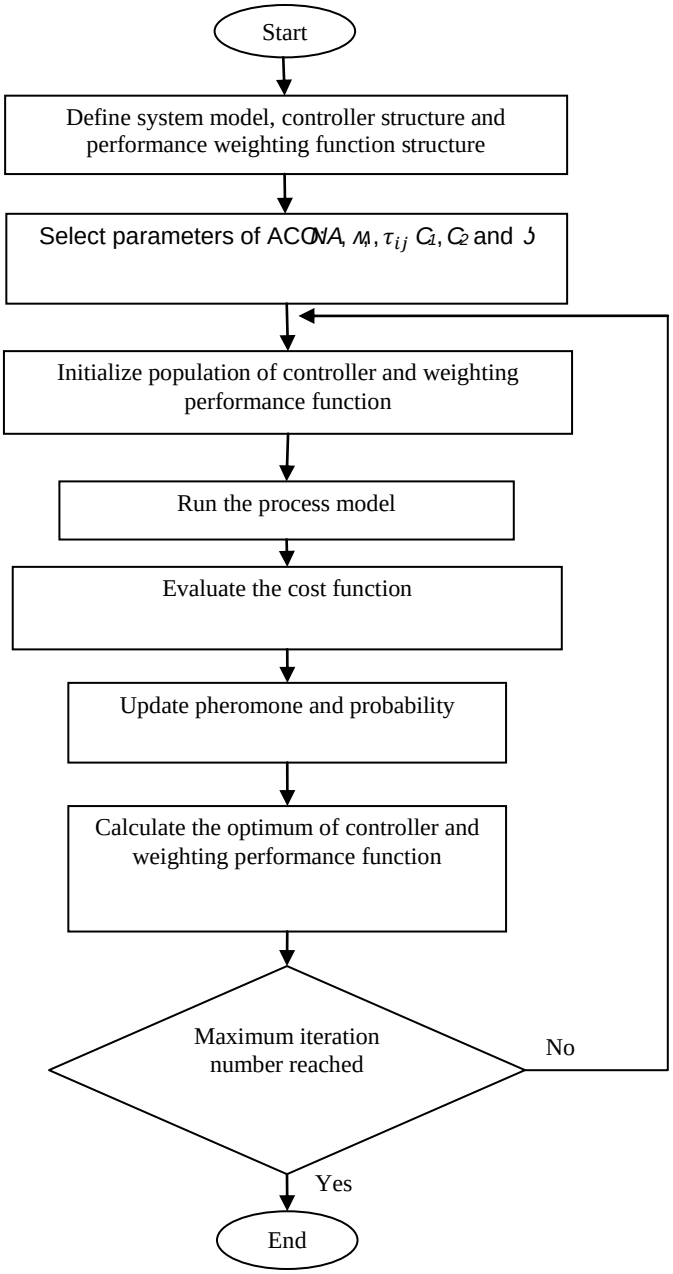

Figure 3 Flowchart of ACO algorithm for obtaining state feedback gains

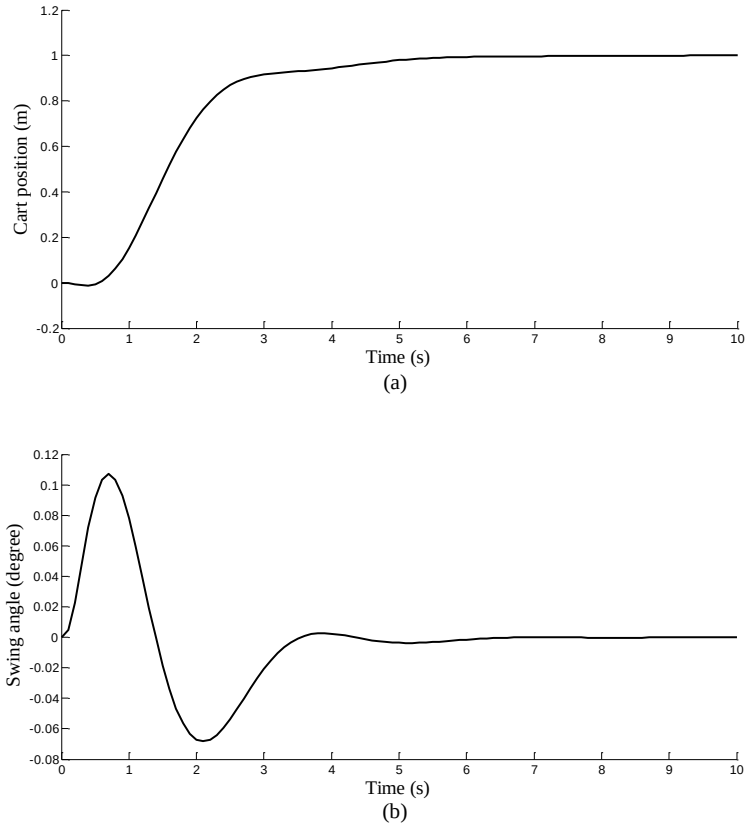

Figure 4 Response of the system using the first proposed cost function (a) cart position (b) swing angle

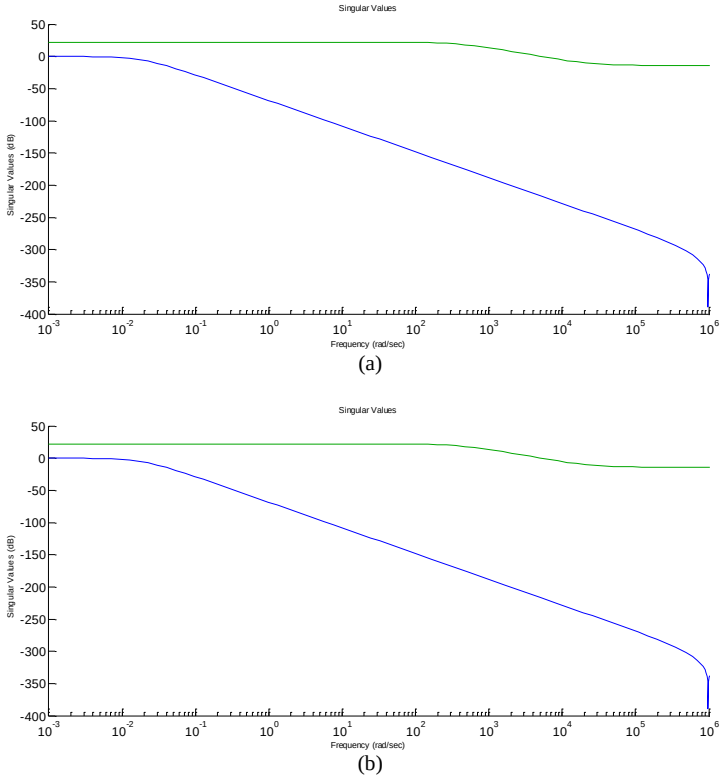

Figure 5 The resulting complementary sensitivity function and sensitivity function (a) *T* with inv(*W*1) (b) *S* with inv (*W*2)

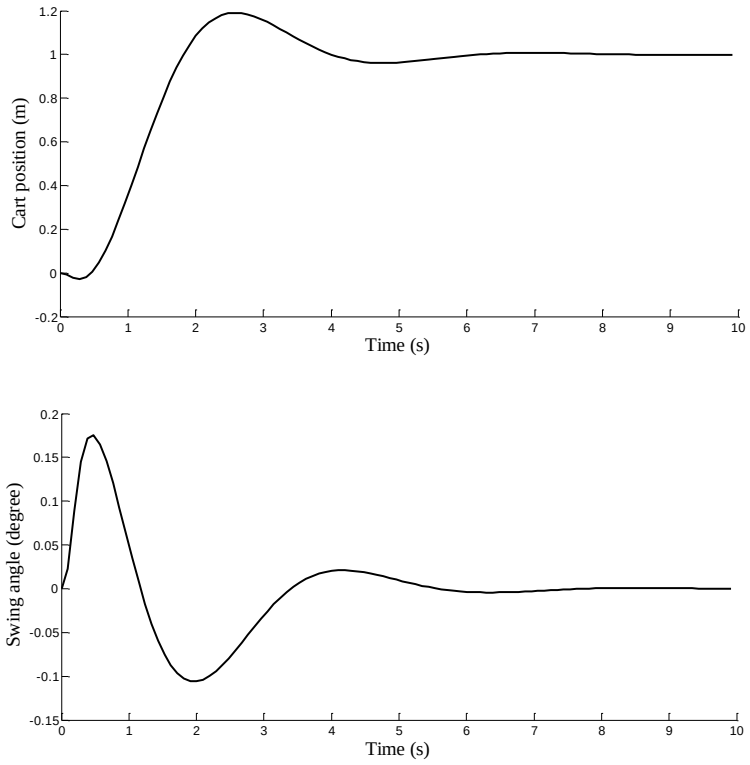

Figure 6 Response of the system using the second proposed cost function (a) cart position (b) swing angle

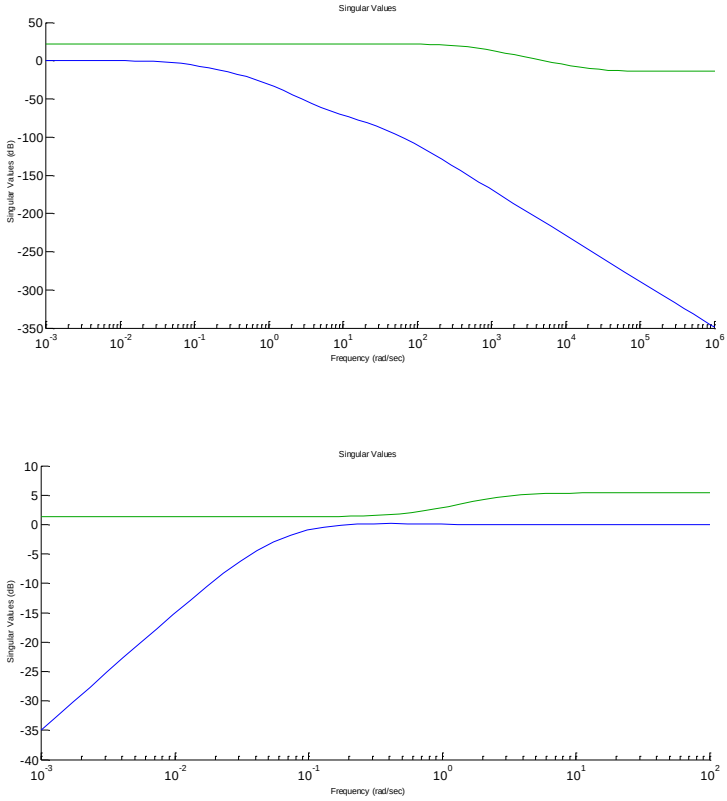

Figure 7 The resulting complementary sensitivity function and sensitivity function (a) *T* with inv(*W*1) (b) *S* with inv(*W*2)

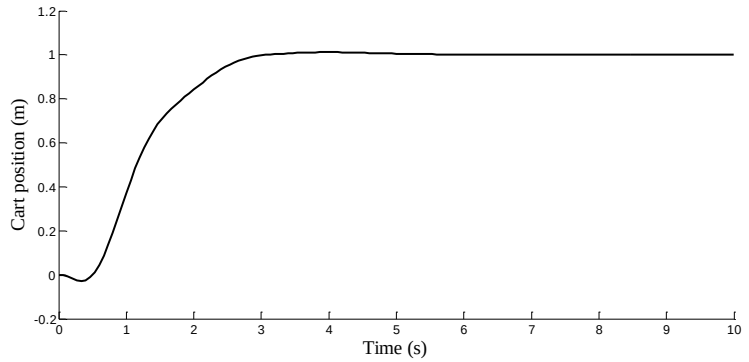

(a)

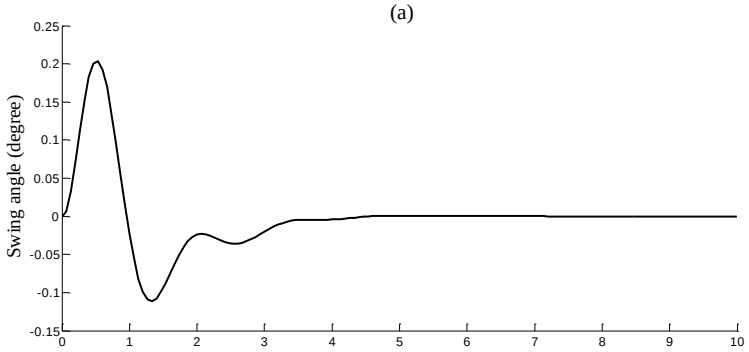

(b)

Figure 8 Response of the system using the third proposed cost function(a) cart position (b) swing angle.

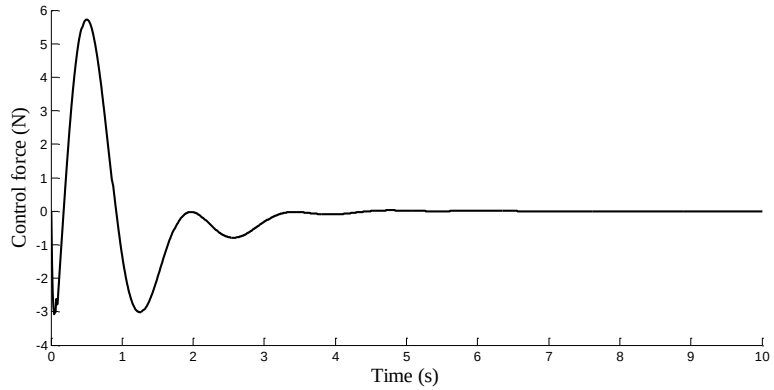

Figure 9 Control signal

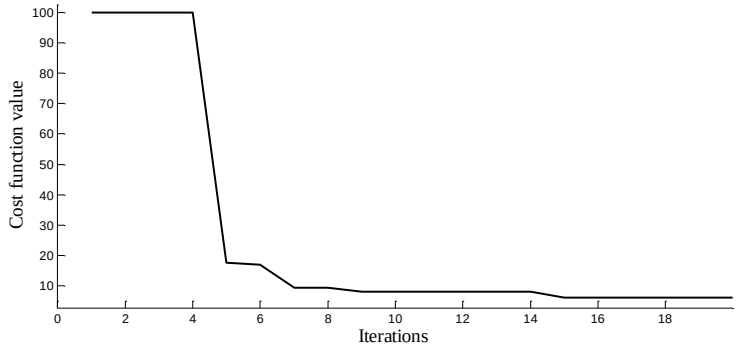

Figure 10 Convergence rate of ACO method

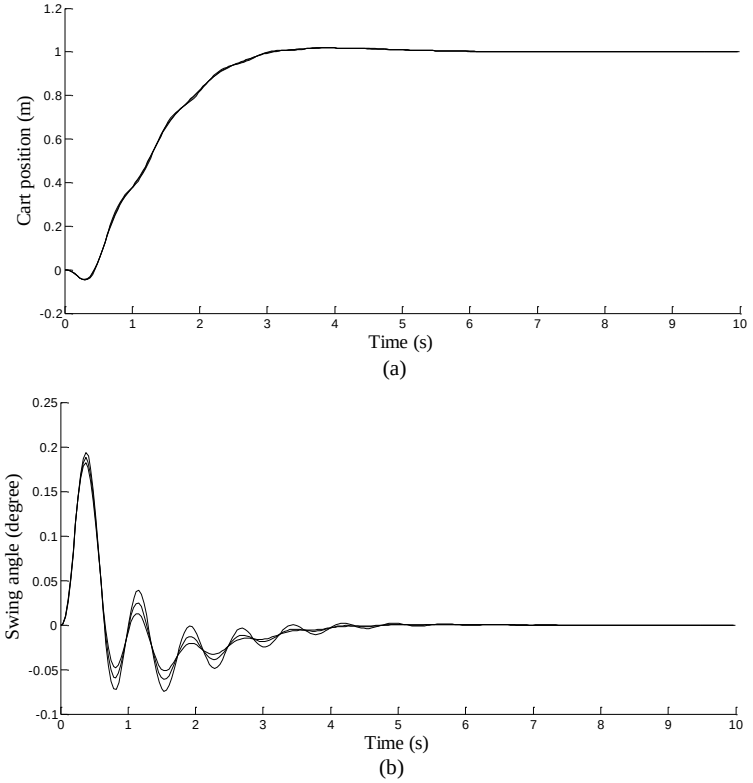

Figure 11 Response of the system with different values of cart mass (a) cart position (b) swing angle

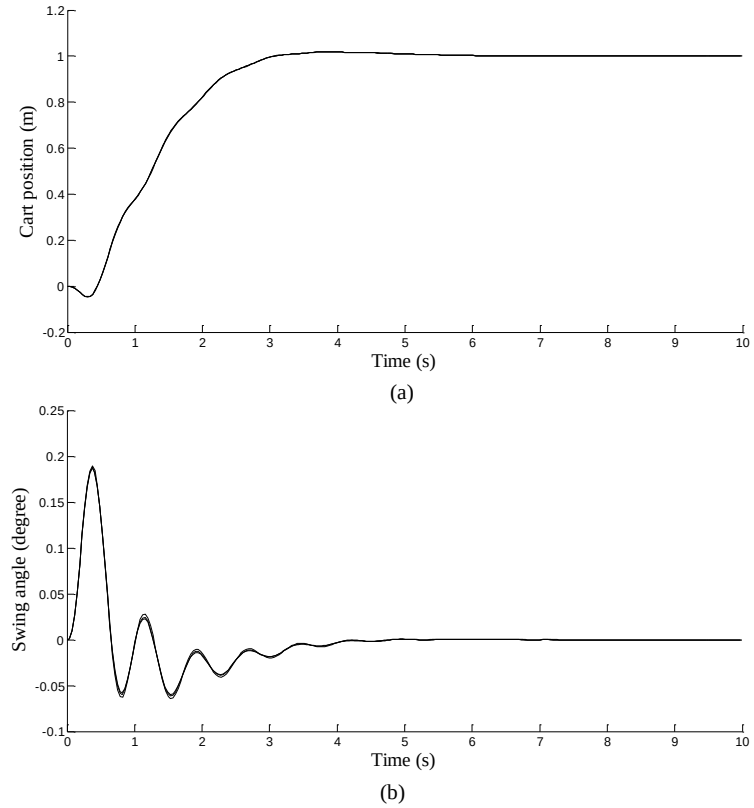

Figure 12 Response of the system with different values of pole mass (a) Cart position (b) swing angle

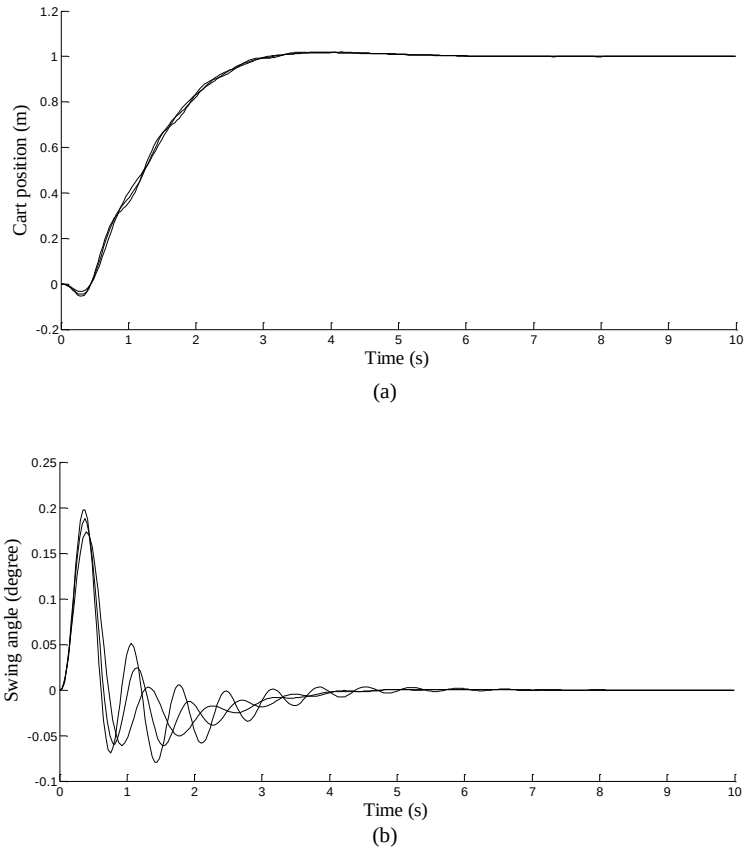

Figure 13 Response of the system with different values of pole length (a) cart position (b) swing angle

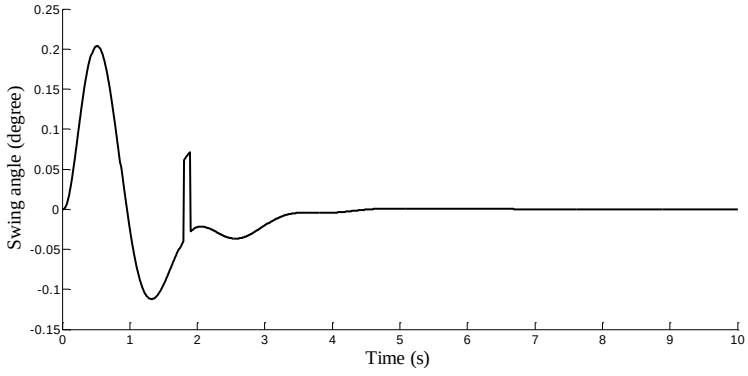

Figure 14 Swing angle when an external disturbance is applied

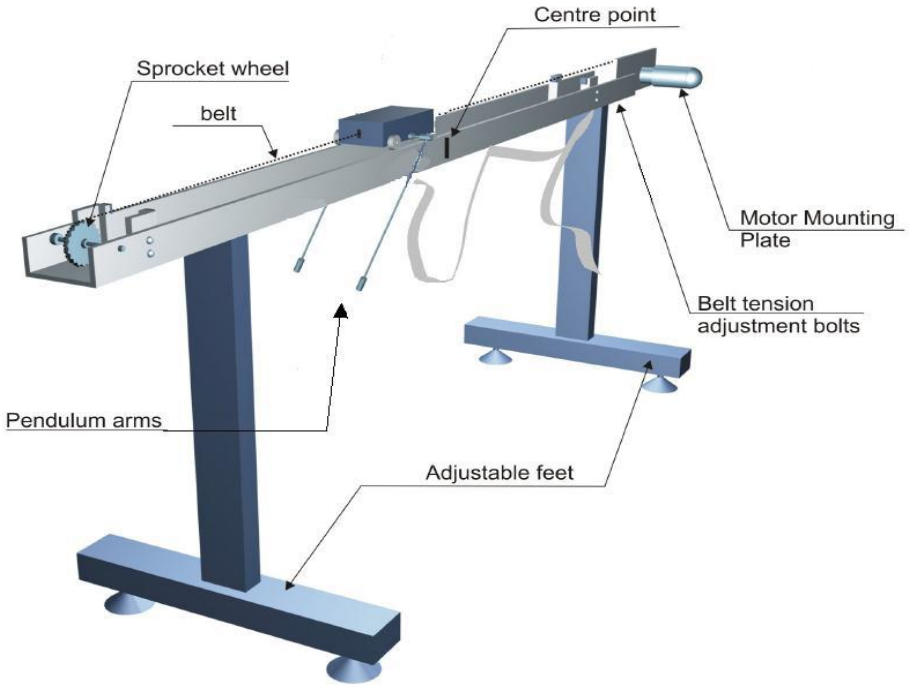

Figure 15 Real inverted pendulum used in this work [11]

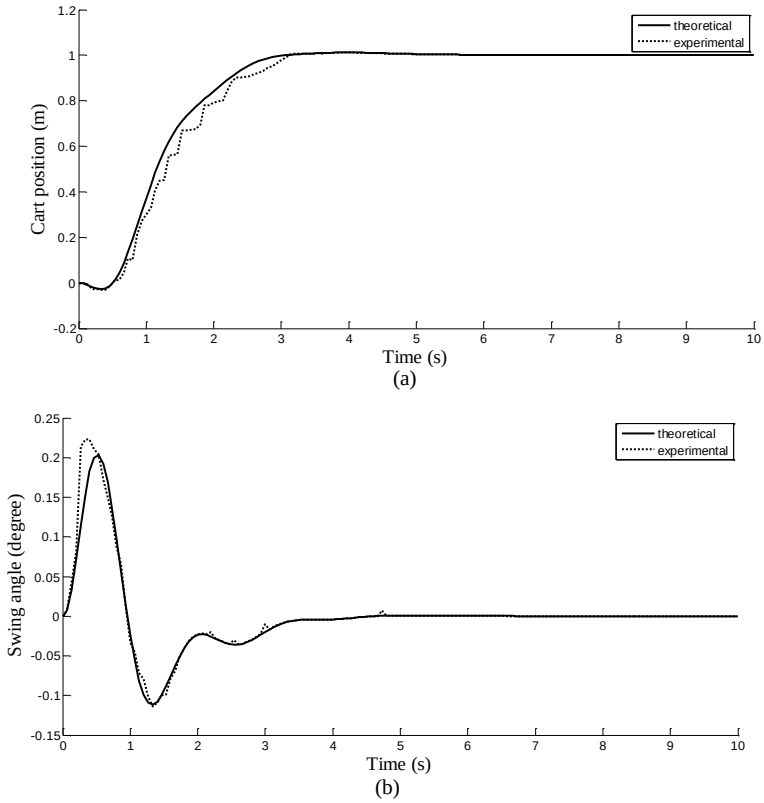

Figure 16 Comparison between theoretical and experimental responses (a) cart position (b) swing angle

Table 2 Performance comparison

Controller	Rise time(s)	Settling time (s)	Percent overshoot
LQR [6]	1.8	3.2	8
Proposed controller	2.3	2.9	zero

References

[1] H. Yu, Y. Liu, T. Yang. 2008.Closed Loop Tracking Control of a Pendulum-Driven Cart-Pole Underactuated System. *Journal of Systems and Control Engingeering*. 222(2): 109–125.

[2] H. L. Bui, D. T. Tran, N. L. Vu. 2011. Optimal Fuzzy Control of an Inverted Pendulum. *Journal of Vibration and Control*. 18(14): 2097–2110.

[3] Y. F. Chen, A. C. Huang. 2014. Adaptive Control of Rotary Inverted Pendulum System with Time-Varying Uncertainties. *Nonlinear Dynamics*. 76: 95–102.

[4] T. C. Kuo, Y. J. Huang, P. C. Wu. 2013. Genetic Algorithm Tuned Fuzzy Logic Controller for Rotary Inverted Pendulum. *Research Journal of Applied Sciences, Engineering and Technology*. 6(5): 907–9013.

[5] O. Boubaker. 2013. The Inverted Pendulum Benchmark in |Nonlinear Control Theory: A Survey. *International Journal of Advanced Robotic Systems*. 10: 1–9.

[6] Hyperlink http://en.wikipedia.org/wiki/Inverted_pendulum (2013). V. Kumar, J. Jerome. 2013. Robust LQR Controller Design for Stabilizing and Trajectory Tracking of Inverted Pendulum, Elsevier. *Procedia Engineering*. 64: 169–178.

[7] P. Bhavsar, V. Kumar. 2012. Trajectory Tracking of Linear Inverted Pendulum using Integral Sliding Mode Control. *International Journal of Intelligent Systems and Applications*. 6: 31–38.

[8] I. Chiha and P. Borne. 2010. Multi-Objective Ant Colony Optimization to Tuning PID Controller. Communication Control and Computing Technologies (ICCCCT). *IEEE International Conference on. IEEE*. 3(2).

[9] B. Nagaraj and P. Vijayakumar. 2011. A Comparative Study of PID Controller Tuning using GA, EP, PSO and ACO. *Journal of Automation, Mobile Robotics & Intelligent Systems Articles*. 5(2).

[10] I. Chiha, N. Liouane and P. Borne. 2012. Tuning PID Controller Using Multiobjective Intelligence and Soft Computing. 2.

[11] K. Chakraborty, R. R. Mukherjee, S. Mukherjee. 2013. Tuning of PID Controller of Inverted Pendulum using Genetic Algorithm. *International Journal of Soft Computing and Engineering*. 3(1): 21–24.

[12] P. Kumar, O. N. Mehrotra, J. Mahto. 2012. Controller Design of Inverted Pendulum using Pole Placement and LQR. *IJRET*. 1(4): 532–538,

[13] A. Roshdy, Y. Z. Lin, H. F. Mokbel, T. Wang. 2012. Stabilization of Real Inverted Pendulum using Pole Separation Factor. *Proceedings of International Conference on Mechanical Engineering and Material Science*.

[14] Digital Inverted Pendulum Control Experiments, 33-936S, Feedback Instruments Ltd. UK.

[15] F. Faizan, F. Farid, M. Rehan, and *et al*. 2010. Implementation of Discrete PID on Inverted Pendulum. 2nd International Conference on Education Technology and Computer (ICETC). 1(1): 48–51.

[16] Y. Lan and M. Fei. 2011. Design of State-Feedback Controller by Pole Placement for a Coupled Set of Inverted Pendulums. 10th International Conference on Electronic Measurement and Instruments (ICEMI). 3: 69–73.

[17] K. Ogata. 2010. *Modern Control Engineering*. 5th Edition. Prentice Hall.